

Improvement in Hydrogenation and Dehydrogenation Characteristics of Magnesium by Addition of Titanium (III) Chloride via Transformation-Accompanying Milling

Myoung Youp SONG^{1*}, Seong Ho LEE², Young Jun KWAK², Hye Ryoung PARK³

¹ Division of Advanced Materials Engineering, Hydrogen & Fuel Cell Research Center, Engineering Research Institute, Chonbuk National University, 567 Baekje-daero Deokjin-gu Jeonju, 54896, Republic of Korea

² Department of Materials Engineering, Graduate School, Chonbuk National University, 567 Baekje-daero Deokjin-gu Jeonju, 54896, Republic of Korea

³ School of Applied Chemical Engineering, Chonnam National University, 77 Yongbong-ro Buk-gu Gwangju, 61186, Republic of Korea

crossref <http://dx.doi.org/10.5755/j01.ms.23.3.16375>

Received 07 October 2016; accepted 06 December 2016

A specimen consisting of 90 wt.% Mg and 10 wt.% TiCl₃ (called 90 Mg + 10 TiCl₃) was made by transformation-accompanying milling, and its hydrogenation and dehydrogenation features were checked. The activation of 90 Mg + 10 TiCl₃ was not demanded. 90 Mg + 10 TiCl₃ revealed an useful hydrogenation-dehydrogenation capacity (the quantity of hydrogen absorbed in 60 min) of about 5.6 wt.%. At C_n = 1, the specimen absorbed 4.06 wt.% of hydrogen in 5 min, 5.09 wt.% of hydrogen in 10 min, and 5.59 wt.% of hydrogen in 60 min at 593 K in 1.2 MPa H₂. At C_n = 1, the specimen desorbed 0.47 wt.% of hydrogen in 2.5 min, 3.81 wt.% of hydrogen in 30 min, and 5.20 wt.% of hydrogen in 60 min at 593 K in 0.1 MPa H₂. The XRD pattern of 90 Mg + 10TiCl₃ dehydrogenated at the 4th hydrogenation-dehydrogenation cycle included Mg, β-MgH₂, MgO, and a small amount of TiH_{1.924} phases. The P (equilibrium hydrogen pressure)-C (composition)-T (temperature) curve at 593 K revealed an equilibrium plateau pressure at about 0.25 MPa. 90 Mg + 10 TiCl₃ had a higher early hydrogenation rate and a larger amount of hydrogen absorbed in 60 min than Mg, 90 Mg + 10 Fe₂O₃, 90 Mg + 10 MnO, and 90 Mg + 10 TaF₅, the hydrogenation and dehydrogenation features of which were before informed of.

Keywords: hydrogen storage, magnesium-based alloys, transformation-accompanying milling, hydrogen sorption rates.

1. INTRODUCTION

The storage of hydrogen using metal hydrides as hydrogenation and dehydrogenation media has several strengths over storage by compression, storage by liquefaction, and storage by adsorption with carbon nanotube: metal hydrides own a higher hydrogenation and dehydrogenation capacity on the basis of volume and hydrogen storage by metal hydrides is safer than storage by compression and storage by liquefaction. To release hydrogen out of metal hydrides, squandered heat can be employed. Besides, selective hydrogen storage and release of metal hydrides enables us to produce hydrogen with high purity [1].

Magnesium owns a high hydrogenation and dehydrogenation capacity (7.6 wt.%), is of relatively low price, and has a great deal of deposit in the earth's crust. However, it has low hydrogenation and dehydrogenation rates. Much research to heighten the hydrogenation and dehydrogenation rates of magnesium has been conducted by preparing magnesium and transition metal alloys [2] such as Pd [3], Ni [4], Sm [5], Ni and B [6], Pr and Ni [7], and Sc, Ti, V, Cr, Y, Zr, Nb, and Mo [8], and by making magnesium and transition metal compounds like Mg₁₇Ba₂ [9].

Ma et al. [10] reported that TiF₃ improved the

absorption/desorption kinetics of magnesium hydride (MgH₂) superiorly over TiCl₃. Both TiF₃ and TiCl₃ additives generated highly dispersed active TiH₂ phase and inactive magnesium halides. The reaction of TiCl₃ with MgH₂ produced TiH₂ and MgCl₂.

Magnesium hydride milled with different halides was prepared by Malka et al. [11] to check the optimum percentage of added halide and preparing conditions. They investigated the influences of these added halides on the dehydrogenation temperature of MgH₂ and the decrease in activation energy for dehydrogenation. Catalytic efficiencies of the chlorides and fluorides of the different metallic elements in the samples were compared. Considering electronic states of the metals in selected halides, the effects of the selected halides on MgH₂ decomposition temperature were also discussed. They informed of that TiCl₃ was one of the halides with the best catalytic effects for the dehydrogenation of magnesium hydride, among the studied halides.

The influence of 7 wt.% dopants, such as ZrF₄, TaF₅, NbF₅ and TiCl₃, on the kinetics of absorption and desorption of magnesium hydride was studied by Malka et al. [12]. They reported that the valence state of the metal halides changed during processing and NbF₅, TaF₅ and particularly TiCl₃, took part in the disproportionation reactions that created a significant amount of structural defects.

*Corresponding author. Tel.: +82-63-270-2379; fax: +82-63-270-2386.
E-mail address: songmy@jbnu.ac.kr (M.Y. Song)

In the present study, TiCl_3 was picked for additive to heighten of hydrogenation and dehydrogenation rates of Mg. Mg was used as a starting material because it is less expensive than MgH_2 . The preparation of MgH_2 is quite hard; it requires high hydrogen pressures and long periods. In our previous works [13, 14], the best percentage of additives, to improve hydrogenation and dehydrogenation features of Mg, was about ten. A specimen consisting of 90 wt.% Mg and 10 wt.% TiCl_3 , which includes 10 wt.% additive, was prepared by transformation-accompanying milling. The conditions for optimum transformation-accompanying milling, which were studied in our previous works [15, 16], were used for the preparation of specimens. Its hydrogenation and dehydrogenation features such as hydrogenation and dehydrogenation rates and P-C-T (equilibrium hydrogen pressure-composition-temperature) curve, were then studied. Hydrogenation was done under a relatively low hydrogen pressure (1.2 MPa H_2) and dehydrogenation under a relatively high hydrogen pressure (0.1 MPa H_2), compared with the hydrogen pressures applied in other works for the hydrogenation and dehydrogenation features of metal hydrides. We designated the specimen consisting of 90 wt.% Mg and 10 wt.% TiCl_3 as 90 Mg + 10 TiCl_3 . The hydrogenation and dehydrogenation properties of 90 Mg + 10 TiCl_3 were compared with those of oxide-added specimens, such as 90 Mg + 10 Fe_2O_3 and 90 Mg + 10 MnO , and 90 Mg + 10 TaF_5 which were reported before.

2. EXPERIMENTAL DETAILS

Pure Mg powder (particle size 74–149 μm , purity 99.6 %, Alfa Aesar), and TiCl_3 (Titanium (III) chloride, Aldrich) were utilized as the initiating substances.

Specimens were got ready in an argon atmosphere. Transformation-accompanying milling was performed at 250 rpm in a ball mill (Planetary Mono Mill; Pulverisette 6, Fritsch) in about 1.2 MPa H_2 . A 90 wt.% Mg and 10 wt.% TiCl_3 mixture with a weight of 8 g was mixed with 105 hardened steel balls of a total weight of 360 g in a sealed 250 ml container made of stainless steel. The milling time was 6 h by iterating milling for 15 min and resting for 5 min. Hydrogen was replenished every 2 h.

The amount of hydrogen absorbed or desorbed was quantified as the hydrogenation or dehydrogenation reaction proceeds, using a Sievert-type volumetric hydrogenation and dehydrogenation apparatus [17]. During quantifying the amount of hydrogen absorbed or desorbed, the hydrogen pressure was maintained nearly constant by making up the absorbed hydrogen from a small reservoir of a measured volume during hydrogenation or taking out the desorbed hydrogen to the small reservoir during dehydrogenation. The weight of the specimen utilized for these measurements was 0.5 g. After the absorbed and then desorbed hydrogen quantities were measured at 593 K under 1.2 and 0.1 MPa H_2 for 1 h, respectively, the specimen was then dehydrogenated at 623 K in vacuum for 2 h. The P (equilibrium hydrogen pressure)-C (composition)-T (temperature) curve was obtained by repeating waiting for equilibrium and then measuring equilibrium hydrogen pressure and taking some hydrogen out of the reactor and then measuring the taken hydrogen

quantity.

The phases in the specimens after transformation-accompanying milling and after hydrogenation-dehydrogenation cycling were analyzed by X-ray diffraction (XRD) with Cu $\text{K}\alpha$ radiation in a powder diffractometer (Rigaku D/MAX 2500). Scanning electron microscope (SEM) micrographs of the specimens were obtained in a JSM-5900 SEM operated at 15 kV.

3. RESULTS AND DISCUSSION

The XRD diagram of 95 Mg + 10 TiCl_3 after transformation-accompanying milling showed that the specimen included Mg, $\beta\text{-MgH}_2$, and small quantities of $\gamma\text{-MgH}_2$ and $\text{TiH}_{1.924}$ phases. $\beta\text{-MgH}_2$ and $\gamma\text{-MgH}_2$ were built by the combination of Mg with hydrogen during transformation-accompanying milling. $\beta\text{-MgH}_2$ and $\gamma\text{-MgH}_2$ are low-pressure and high-pressure forms of MgH_2 , respectively, each being belong to tetragonal and orthorhombic crystal systems. The combination of Ti with hydrogen during transformation-accompanying milling also led to the development of $\text{TiH}_{1.924}$.

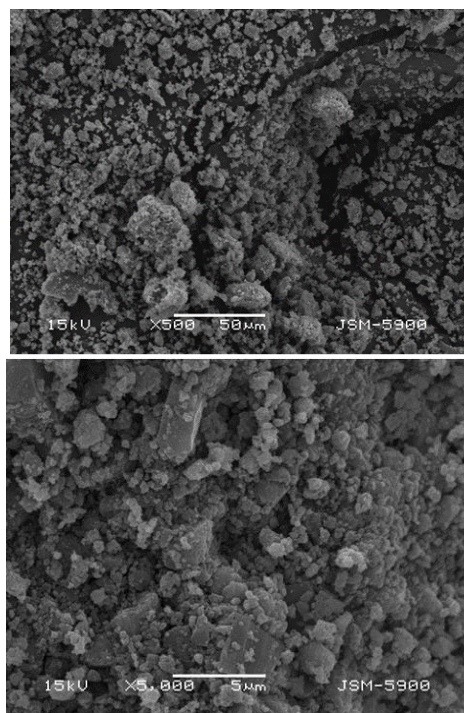


Fig. 1. SEM micrographs of 90 Mg + 10 TiCl_3 after transformation-accompanying milling

SEM micrographs of 90 Mg + 10 TiCl_3 after transformation-accompanying milling are exhibited in Fig. 1. The particle sizes are not homogeneous and the shapes of particles are irregular. Small particles are also observed on the surfaces of the relatively large particles. Some big particles have smooth surfaces. Agglomerates are also found.

The percentage of hydrogenated hydrogen, H_a , is defined as $100 \times (\text{the weight of hydrogenated hydrogen} / \text{the sample weight})$. The change in the H_a vs. t curve at 593 K in 1.2 MPa H_2 according to the number of hydrogenation-dehydrogenation cycles, C_n , for 90 Mg + 10 TiCl_3 is shown in Fig. 2. At the first cycle, the hydrogenation rate is very high from the starting to 5 min

around, and then severely low after 10 min. It is believed that the very high hydrogenation rate until 5 min is due to hydrogen absorption by small particles, small particles on the surfaces of large particles, and outer sides, which have many hydrogen paths such as cracks, of large particles and agglomerates. The very low hydrogenation rate after 10 min is probably resulted from the absorption of hydrogen by the insides of particles, which can be hydrogenated after diffusion of hydrogen through growing hydride layers. As the number of hydrogenation-dehydrogenation cycles increases from $C_n = 1$ to $C_n = 3$, the early hydrogenation rate increases and the amount of hydrogen absorbed in 60 min decreases. At $C_n = 1$, the sample absorbs 4.06 wt.% of hydrogen in 5 min, 5.09 wt.% of hydrogen in 10 min, 5.57 wt.% of hydrogen in 30 min, and 5.59 wt.% of hydrogen in 60 min. The useful hydrogenation-dehydrogenation capacity is defined as the quantity of hydrogen absorbed in 60 min. 90 Mg + 10 TiCl₃ has a useful hydrogenation-dehydrogenation capacity of about 5.6 wt.% at $C_n = 1$. Table 1 presents the change in the absorbed hydrogen quantity with time for 90 Mg + 10 TiCl₃ at 593 K in 1.2 MPa H₂ at $C_n = 1 - 3$.

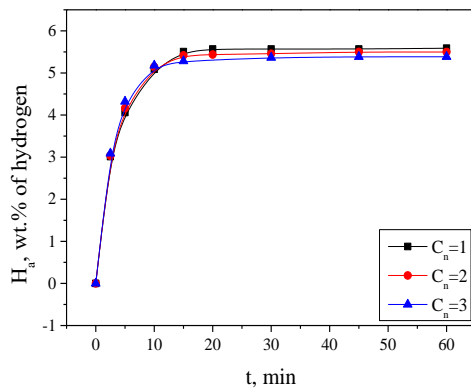


Fig. 2. Change in the H_a vs. t curve at 593 K in 1.2 MPa H₂ according to the number of hydrogenation-dehydrogenation cycles, C_n , for 90Mg+10TiCl₃

Table 1. Change in the absorbed hydrogen quantity with time for 90 Mg + 10 TiCl₃ at 593 K in 1.2 MPa H₂ at $C_n = 1 - 3$

	Absorbed hydrogen quantity (wt.% of hydrogen)				
	2.5 min	5 min	10 min	30 min	60 min
$C_n = 1$	3.01	4.06	5.09	5.57	5.59
$C_n = 2$	3.03	4.16	5.15	5.46	5.50
$C_n = 3$	3.09	4.32	5.18	5.37	5.38

Fig. 3 shows the changes in the early hydrogenation rate and the quantity of hydrogen absorbed in 60 min, H_a (60 min), with the number of hydrogenation-dehydrogenation cycles, C_n , at 593 K in 1.2 MPa H₂ for 90 Mg + 10 TiCl₃. As C_n increases, the early hydrogenation rate increases, whereas H_a (60 min) decreases. The increase in the early hydrogenation rate with hydrogenation-dehydrogenation cycling is believed due to decrease in size of the particles on the surface. The decrease in H_a (60 min) with hydrogenation-dehydrogenation cycling is thought owing to sintering of the particles inside the particles and agglomerates.

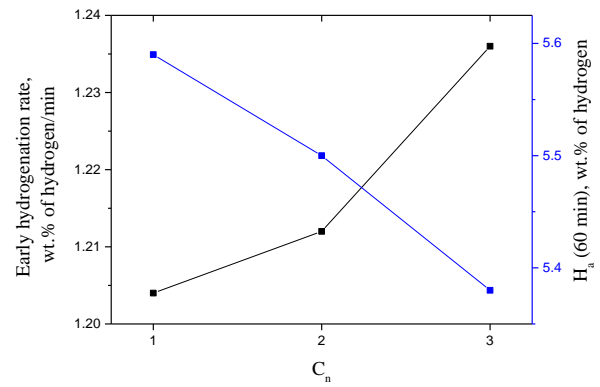


Fig. 3. Changes in the early hydrogenation rate and the quantity of hydrogen absorbed in 60 min, H_a (60 min), with the number of hydrogenation-dehydrogenation cycles, C_n , at 593 K in 1.2 MPa H₂ for 90 Mg + 10 TiCl₃

The percentage of desorbed hydrogen, H_d , is defined as $100 \times$ (the weight of desorbed hydrogen / the sample weight). The change in the H_d vs. t curve at 593 K in 0.1 MPa H₂ according to the number of hydrogenation-dehydrogenation cycles, C_n , for 90 Mg + 10 TiCl₃ is shown in Fig. 4.

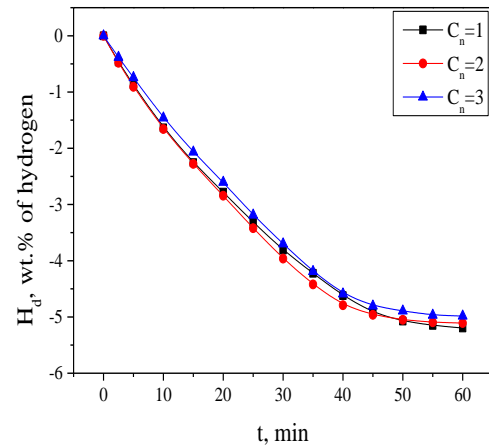


Fig. 4. Change in the H_d vs. t curve at 593 K in 0.1 MPa H₂ according to the number of hydrogenation-dehydrogenation cycles, C_n , for 90 Mg + 10 TiCl₃

Table 2. Change in the desorbed hydrogen quantity with time for 90 Mg + 10 TiCl₃ at 593 K in 0.1 MPa H₂ at $C_n = 1 - 3$

	Desorbed hydrogen quantity (wt.% of hydrogen)				
	2.5 min	5 min	10 min	30 min	60 min
$C_n = 1$	0.47	0.88	1.64	3.81	5.20
$C_n = 2$	0.48	0.91	1.66	3.96	5.11
$C_n = 3$	0.38	0.74	1.46	3.70	4.98

The specimen has a slightly higher early dehydrogenation rates at $C_n = 2$ than at $C_n = 1$, and the early dehydrogenation rate at $C_n = 3$ is lower than at $C_n = 2$ and $C_n = 1$. At $C_n = 1$, the specimen desorbs 0.47 wt.% of hydrogen in 2.5 min, 3.81 wt.% of hydrogen in 30 min, and 5.20 wt.% of hydrogen in 60 min. At $C_n = 1$, the quantity of hydrogen desorbed in 60 min is 93 % of that absorbed in 60 min. The quantity of hydrogen desorbed in 60 min decreases as the number of hydrogenation-dehydrogenation cycles increases from 1 to 3. Table 2

presents the change in the desorbed hydrogen quantity with time for 90 Mg + 10 TiCl₃ at 593 K in 0.1 MPa H₂ at C_n = 1 – 3.

Fig. 5 shows the changes in the early dehydrogenation rate and the quantity of hydrogen desorbed in 60 min, H_d (60 min), with the number of hydrogenation-dehydrogenation cycles, C_n, at 593 K in 1.2 MPa H₂ for 90 Mg + 10 TiCl₃. As C_n increases, the early dehydrogenation rate increases at C_n = 2 and decreases at C_n = 3. The early dehydrogenation rate at C_n = 3 is lower than at C_n = 2 and C_n = 1. H_d (60 min) decreases as C_n increases from 1 to 3.

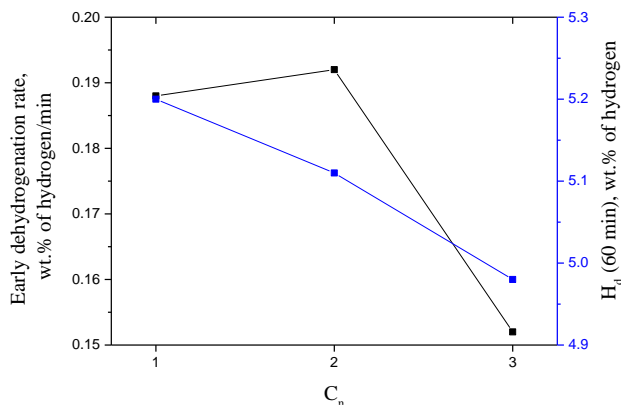


Fig. 5. Changes in the early dehydrogenation rate and the quantity of hydrogen desorbed in 60 min, H_d (60 min), with the number of hydrogenation-dehydrogenation cycles, C_n, at 593 K in 1.2 MPa H₂ for 90 Mg + 10 TiCl₃

Activation is a process which makes the sample have maximum reaction rates. For metal hydrides, it is performed by hydrogenation-dehydrogenation cycling. Fig. 2 – Fig. 5 show that the activation of 90 Mg + 10 TiCl₃ is not demanded.

The XRD diagram of 90 Mg + 10 TiCl₃ dehydrogenated at the 4th hydrogenation-dehydrogenation cycle showed that the sample included Mg, β-MgH₂, MgO, and a small amount of TiH_{1.924} phases. TiH_{1.924}, which was formed after transformation-accompanying milling, was not dehydrogenated even after dehydrogenation at 623 K in vacuum for 2 h. Titanium hydride (TiH₂) was also reported to form in the dehydrogenated MgH₂ + 4 mol % TiCl₃ of Ma et al.'s work [10]. This XRD diagram exhibited slightly narrower peaks and lower background than the XRD diagram of 90 Mg + 10 TiCl₃ after transformation-accompanying milling. This suggests that this specimen has better crystallinity than the specimen after transformation-accompanying milling.

The SEM micrographs of 90 Mg + 10 TiCl₃ dehydrogenated at the 4th hydrogenation-dehydrogenation cycle are shown in Fig. 6. This specimen has particles of various sizes with a large number of small particles on their surfaces. Smooth surfaces of some big particles disappeared and small particles are found on the large particles. Particles are agglomerated. The particles on the surfaces are finer but the size of agglomerates is larger as compared with those after transformation-accompanying milling.

Fig. 7 shows a dehydrogenation P-C-T (equilibrium hydrogen pressure-composition-temperature) curve of 90 Mg + 10 TiCl₃ at 593 K.

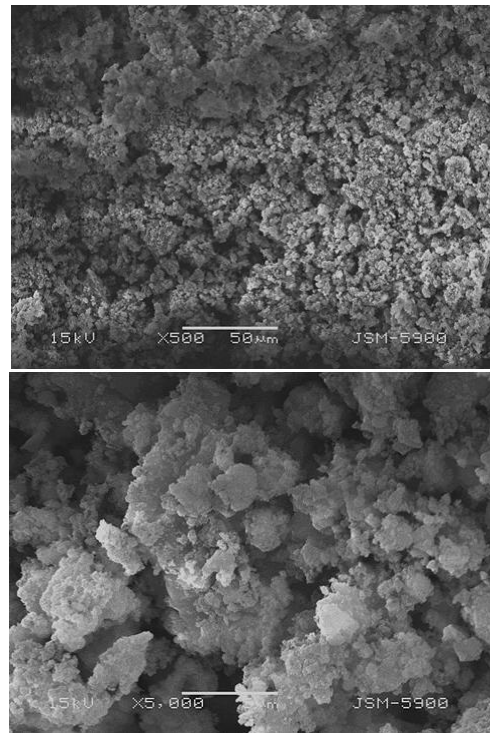


Fig. 6. SEM micrographs of 90Mg+10TiCl₃ dehydrogenated at the 4th hydrogenation-dehydrogenation cycle

The hydrogen pressure decreases abruptly from a hydrogen pressure of about 1.17 MPa to about 0.27 MPa, then maintains almost constant at about 0.25 MPa, and finally decreases slowly. The equilibrium plateau pressure (about 0.25 MPa) is found at an H_d range of 5.0 – 1.0 wt.% of hydrogen. The slope of the equilibrium plateau pressure is believed to appear because other phases, such as titanium hydride (TiH_{1.924}), are present in addition to Mg-H solid solution and magnesium hydride. The 90 Mg + 10 TiCl₃ specimen contains a very small amount of titanium hydride and the main hydride phase of the 90 Mg + 10 TiCl₃ specimen is MgH₂. The equilibrium plateau pressure of about 0.25 MPa for 90 Mg + 10 TiCl₃ at 593 K is very similar to that of the Mg-H system at 593 K reported by Stampfer et al. [18]. The data of Stampfer et al. [18] showed that the equilibrium plateau pressure in the Mg-H system at 593 K is 0.27 MPa. The hydrogen-storage capacity of the sample is about 5.0 wt.%. This sample has an effective hydrogen-storage capacity (the quantity of hydrogen absorbed for 60 min) of about 5.6 wt.%. The hydrogen-storage capacity of the sample is believed to be smaller than the effective hydrogen-storage capacity because the sample was stored for a couple of months in a glove box and slightly contaminated.

In our former research [19], the hydrogenation and dehydrogenation features were investigated for 90 Mg + 10 Fe₂O₃, 90 Mg + 10 Fe₂O₃ got ready by spray conversion, 90 Mg + 10 MnO, and 90 Mg + 10 SiO₂ specimens, which were made by transformation-accompanying milling for 2 h under the milling conditions like those to make 90 Mg + 10 TiCl₃ specimen. 90 Mg + 10 Fe₂O₃ and 90 Mg + 10 MnO had relatively high hydrogenation or dehydrogenation speeds. In another previous work of our group [20], the hydrogenation and dehydrogenation features were investigated for

90 Mg + 10 TaF₅, which were made by transformation-accompanying milling under the milling conditions like those to make 90 Mg + 10 TiCl₃ specimen. 90 Mg + 10 TaF₅ showed quite high hydrogenation and dehydrogenation speeds.

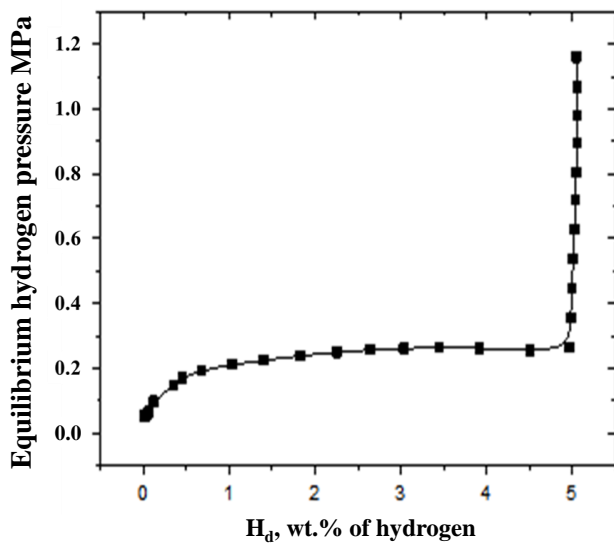


Fig. 7. Dehydrogenation P-C-T (equilibrium hydrogen pressure-composition-temperature) curve of 90 Mg + 10 TiCl₃ at 593 K

The H_a vs. t curves at 593 K in 1.2 MPa H₂ at C_n=1 for 90 Mg + 10 TiCl₃, Mg [21], 90 Mg + 10 Fe₂O₃ [19], 90 Mg + 10 MnO [19], and 90 Mg + 10 TaF₅ [20] were compared. Mg, 90 Mg + 10 Fe₂O₃, 90 Mg + 10 MnO, and 90 Mg + 10 TaF₅ were made under the milling conditions like those to make 90 Mg + 10 TiCl₃ specimen. Mg absorbed hydrogen extremely slowly. 90 Mg + 10 TiCl₃ had a higher early hydrogenation rate and a larger quantity of hydrogen absorbed in 60 min than Mg, 90 Mg + 10 Fe₂O₃, 90 Mg + 10 MnO, and 90 Mg + 10 TaF₅. 90 Mg + 10 TiCl₃ had the highest early hydrogenation rate, followed in a decreasing order by 90 Mg + 10 TaF₅, 90 Mg + 10 Fe₂O₃, 90 Mg + 10 MnO, and Mg. 90 Mg + 10 TiCl₃ had the largest quantity of hydrogen absorbed in 60 min, followed in a decreasing order by 90 Mg + 10 Fe₂O₃, 90 Mg + 10 TaF₅, 90 Mg + 10 MnO, and Mg. 90 Mg + 10 TiCl₃ absorbed 4.06 wt.% of hydrogen in 5 min, 5.09 wt.% of hydrogen in 10 min, 5.57 wt.% of hydrogen in 30 min, and 5.59 wt.% of hydrogen in 60 min. 90 Mg + 10 Fe₂O₃ absorbed 2.41 wt.% of hydrogen in 2.5 min, 3.52 wt.% of hydrogen in 5 min, 4.26 wt.% of hydrogen in 10 min, 4.84 wt.% of hydrogen in 30 min, and 5.16 wt.% of hydrogen in 60 min. Mg absorbed 0.08 wt.% of hydrogen in 2.5 min, and 0.14 wt.% of hydrogen in 60 min.

The transformation-accompanying milling of Mg with TiCl₃, which forms β-MgH₂, γ-MgH₂, and TiH_{1.924} is thought to produce defects on the surface and inside Mg particle, to make new clean surfaces, and to curtail the Mg particle sizes. Producing of defects makes easy nucleation of magnesium hydride, making of new clean surfaces increases the reactivity of particles with hydrogen, and reduction in the Mg particle sizes shortens diffusion distances of hydrogen atoms. These effects increase the

hydrogenation and dehydrogenation rates of Mg. The formed β-MgH₂, γ-MgH₂, and TiH_{1.924} are considered to make these effects stronger.

The higher early hydrogenation rates of 90 Mg + 10 TiCl₃ and 90 Mg + 10 TaF₅ than those of 90 Mg + 10 Fe₂O₃ and 90 Mg + 10 MnO indicate that the effects of the addition of halides on the increase in the hydrogenation rates of Mg are stronger than those of the addition of oxides.

4. CONCLUSIONS

The activation of 90 Mg + 10 TiCl₃ was not demanded. 90 Mg + 10 TiCl₃ had a useful hydrogenation-dehydrogenation capacity of about 5.6 wt.%. At C_n=1, the specimen absorbed 4.06 wt.% of hydrogen in 5 min, 5.09 wt.% of hydrogen in 10 min, 5.57 wt.% of hydrogen in 30 min, and 5.59 wt.% of hydrogen in 60 min at 593 K in 1.2 MPa H₂. At C_n=1, the specimen desorbed 0.47 wt.% of hydrogen in 2.5 min, 3.81 wt.% of hydrogen in 30 min, and 5.20 wt.% of hydrogen in 60 min at 593 K in 0.1 MPa H₂. γ-MgH₂ was formed in 90 Mg + 10 TiCl₃ after transformation-accompanying milling. TiH_{1.924}, which was formed after transformation-accompanying milling, was not dehydrogenated even after dehydrogenation at 623 K in vacuum for 2 h. As the number of hydrogenation-dehydrogenation cycles increased from C_n=1 to C_n=3, the early hydrogenation rate increased due to decrease in size of the particles on the surface and the quantity of hydrogen absorbed in 60 min decreased due to sintering of the particles inside the particles and agglomerates. The P-C-T curve at 593 K showed an equilibrium plateau pressure at about 0.25 MPa. 90 Mg + 10 TiCl₃ had a higher early hydrogenation rate and a larger quantity of hydrogen absorbed in 60 min than 90 Mg + 10 TaF₅, 90 Mg + 10 Fe₂O₃, 90 Mg + 10 MnO, and Mg, the hydrogenation and dehydrogenation features of which were before informed of.

Acknowledgements

This research was supported by Basic Science Research Program through the National Research Foundation (NRF) of Korea funded by the Ministry of Education, Science and Technology (Grant number 2011-0023566).

REFERENCES

1. Han, J.S., Kim, S.J., Kim, D.I. A Study of the Pressure-Composition-Temperature Curve of Mg(BH₄)₂ by Sievert's Type Apparatus *Korean Journal of Metals and Materials* 53 2015: pp. 815–820.
2. Rusman, N.A.A., Dahari, M. A Review on the Current Progress of Metal Hydrides Material for Solid-State Hydrogen Storage Applications *International Journal of Hydrogen Energy* 41 2016: pp. 12108–12126. <https://doi.org/10.1016/j.ijhydene.2016.05.244>
3. Ogawa, S., Fujimoto, T., Mizutani, T., Ogawa, M., Uchiyama, N., Kato, K., Ohta, T., Yoshida, T., Yagi, S. Hydrogen Storage of Binary Nanoparticles Composed of Mg and Pd *International Journal of Hydrogen Energy* 40 2015: pp. 11895–11901.
4. Fujimoto, T., Ogawa, S., Kanai, T., Uchiyama, N., Yoshida, T., Yagi, S. Hydrogen Storage Property of

- Materials Composed of Mg Nanoparticles and Ni Nanoparticles Fabricated by Gas Evaporation Method *International Journal of Hydrogen Energy* 40 2015: pp. 11890–11894.
<https://doi.org/10.1016/j.ijhydene.2016.02.108>
5. **Yuan, Z., Yang, T., Bu, W., Shang, H., Qi, Y., Zhang, Y.** Structure, Hydrogen Storage Kinetics and Thermodynamics of Mg-Base $\text{Sm}_5\text{Mg}_{41}$ Alloy *International Journal of Hydrogen Energy* 41 2016: pp. 5994–6003.
 6. **Shao, H., Asano, K., Enoki, H., Akiba, E.** Fabrication and Hydrogen Storage Property Study of Nanostructured Mg–Ni–B Ternary Alloys *Journal of Alloys and Compounds* 479 2009: pp. 409–413.
<https://doi.org/10.1016/j.jallcom.2008.12.067>
 7. **Zhang, Y., Yuan, Z., Yang, T., Feng, D., Cai, Y., Zhao, D.** An Investigation on Hydrogen Storage Thermodynamics and Kinetics of Pr–Mg–Ni-Based PrMg_{12} -Type Alloys Synthesized by Mechanical Milling *Journal of Alloys and Compounds* 688 2016: pp. 585–593.
 8. **El Khatabi, M., Bhihi, M., Naji, S., Labrim, H., Benyoussef, A., El Kenz, A., Loulidi, M.** Study of Doping Effects with 3d and 4d-Transition Metals on the Hydrogen Storage Properties of MgH_2 *International Journal of Hydrogen Energy* 41 2016: pp. 4712–4718.
<https://doi.org/10.1016/j.ijhydene.2016.01.001>
 9. **Wu, D., Ouyang, L., Wu, C., Gu, Q., Wang, H., Liu, J., Zhu, M.** Phase Transition and Hydrogen Storage Properties of $\text{Mg}_{17}\text{Ba}_2$ Compound *Journal of Alloys and Compounds* 690 2017: pp. 519–522.
 10. **Ma, L.P., Kang, X.D., Dai, H.B., Liang, Y., Fang, Z.Z., Wang, P.J., Wang, P., Cheng, H.M.** Superior Catalytic Effect of TiF_3 over TiCl_3 in Improving the Hydrogen Sorption Kinetics of MgH_2 : Catalytic Role of Fluorine anion *Acta Materialia* 57 2009: pp. 2250–2258.
<https://doi.org/10.1016/j.actamat.2009.01.025>
 11. **Malka, I.E., Czujko, T., Bystrzycki, J.** Catalytic Effect of Halide Additives Ball Milled with Magnesium Hydride *International Journal of Hydrogen Energy* 35 2010: pp. 1706–1712.
 12. **Malka, I.E., Pisarek, M., Czujko, T., Bystrzycki, J.** A Study of the ZrF_4 , NbF_5 , TaF_5 , and TiCl_3 Influences on the MgH_2 Sorption Properties *International Journal of Hydrogen Energy* 36 2011: pp. 12909–12917.
<https://doi.org/10.1016/j.ijhydene.2011.07.020>
 13. **Song, M.Y., Ivanov, E., Darriet, B., Pezat, M., Hagenmuller, P.** Hydriding and Dehydriding Characteristics of Mechanically Alloyed Mixtures Mg-x wt.% Ni (x=5, 10, 25, and 55) *Journal of the Less-Common Metals* 131 1987: pp. 71–79.
[https://doi.org/10.1016/0022-5088\(87\)90502-9](https://doi.org/10.1016/0022-5088(87)90502-9)
 14. **Song, M.Y., Kwak, Y.J., Lee, S.H., Park, H.R.** Increase in the Hydrogen Release Rate of MgH_2 by Grinding in a Hydrogen Atmosphere with Ni Added *Journal of Nanoscience and Nanotechnology* 16 2016: pp. 10508–10514.
 15. **Song, M.Y., Kwon, I.H., Kwon, S.N., Park, C.G., Park, H.R., Bae, J.S.** Preparation of Hydrogen-Storage Alloy Mg–10wt% Fe_2O_3 under Various Milling Conditions *International Journal of Hydrogen Energy* 31 2006: pp.43–47.
<https://doi.org/10.1016/j.ijhydene.2005.03.008>
 16. **Song, M.Y., Kwak, Y.J., Lee, S.H., Park, H.R.** Enhancement of Hydrogen Storage Characteristics of Mg by Addition of Nickel and Niobium (V) Fluoride via Mechanical Alloying *Korean Journal of Metals and Materials* 54 2016: pp. 210–216.
 17. **Kwon, S.N.** Improvement of the Hydrogen absorption and Desorption Kinetics of Mg by Catalytic Effects of Fe_2O_3 and Ni *Thesis of Master of Engineering* Chonbuk National University, Republic of Korea 2008: pp.20–22.
 18. **Stampfer, J.F.Jr., Holley, C.E.Jr., Suttle, J.F.** The Magnesium-Hydrogen System *Journal of American Chemical Society* 82 1959: pp. 3504–3508.
<https://doi.org/10.1021/ja01499a006>
 19. **Song, M.Y., Kwon, I.H., Kwon, S.N., Park, C.G., Hong, S.H., Bae, J.S., Mumm, D.R.** Hydrogen-Storage Properties of Mg-Oxide Alloys Prepared by Reactive Mechanical Grinding *Journal of Alloys and Compounds* 415 2006: pp. 266–270.
 20. **Kwak, Y.J., Lee, S.H., Park, H.R., Song, M.Y.** Hydriding and Dehydriding Reactions of Mg-xTaF_5 (x=0, 5 and 10) Prepared via Reactive Mechanical Grinding *Korean Journal of Metals and Materials* 52 2014: pp. 957–962.
 21. **Song, M.Y., Kwak, Y.J., Lee, S.H., Park, H.R.** Hydrogen Storage Properties of Pure Mg *Korean Journal of Metals and Materials* 52 2014: pp. 293–297.
<https://doi.org/10.3365/KJMM.2014.52.4.293>